Resonant energy scales and local observables in the many-body localized phase

Samuel J. Garratt [1,*] and Sthitadhi Roy [2,3,4,†]

[1]*Department of Physics, University of California, Berkeley, California 94720, USA*
[2]*International Centre for Theoretical Sciences, Tata Institute of Fundamental Research, Bengaluru 560089, India*
[3]*Rudolf Peierls Centre for Theoretical Physics, Oxford University, Parks Road, Oxford OX1 3PU, United Kingdom*
[4]*Physical and Theoretical Chemistry, Oxford University, South Parks Road, Oxford OX1 3QZ, United Kingdom*

We formulate a theory for resonances in the many-body localized (MBL) phase of disordered quantum spin chains in terms of local observables. A key result is to show that there are universal correlations between the matrix elements of local observables and the many-body level spectrum. This reveals how the matrix elements encode the energy scales associated with resonance, thereby allowing us to show that these energies are power-law-distributed. Using these results, we calculate analytically the distributions of local polarizations and of eigenstate fidelity susceptibilities. The first of these quantities characterizes the proximity of MBL systems to noninteracting ones, while the second highlights their extreme sensitivity to local perturbations. Our theoretical approach is to consider the effect of varying a local field, which induces a parametric dynamics of spectral properties. We corroborate our results numerically using exact diagonalization in finite systems.

I. INTRODUCTION

If a many-body quantum system is isolated from its environment, it does not necessarily thermalize. In systems that do thermalize, observables are at late times insensitive to the initial conditions [1–5], which is to say that their fluctuations are small. This behavior is reflected in the resemblance between many-body eigenstates and high-dimensional random vectors, which appear featureless to any local probe. The alternative to this ergodic behavior, arising in the presence of strong disorder, is many-body localization [6–10]. In the many-body localized (MBL) phase, there is memory of local observables even at infinite times. In MBL quantum spin chains, for example, eigenstates feature large local polarizations, and these polarizations vary dramatically both in space and over the ensemble of disorder realizations.

Large fluctuations are also found in dynamics. For this reason, averages often fail to represent accurately the behavior of individual MBL systems. A striking example is found in temporal correlations of local observables, and the associated spectral functions [11]. To characterize the MBL phase, it is therefore necessary to develop a theory for the statistical properties of these quantities. In quantum-mechanical systems, it is natural to do so in the spectral representation, and there the question is whether and how the matrix elements of local observables are related to the level spectrum.

In this work, we show that there are universal correlations between these quantities, and that these correlations are characterized by a power-law distribution of energy scales. From these correlations we determine the statistics of local polar-

izations, and we find that these too are broadly distributed. The fluctuations of physical properties are reflected in the extreme sensitivity of eigenstates to local perturbations, and to investigate this we analytically determine the distribution of eigenstate fidelity susceptibilities in the MBL phase. This quantity has recently been investigated extensively as a probe of integrability breaking and of the onset of quantum chaos [12–18].

The calculations described above are unified by the concept of a many-body resonance [15,19–22]. Many-body resonances are generalizations of the Mott resonances that arise in Anderson insulators [23–25], and their presence demarcates MBL systems from their noninteracting counterparts. These resonances control the low-frequency dynamics in the MBL phase [15,19,22,26], and their local structure is central in our understanding of both its stability [15,27] and its breakdown [21,28,29]. One possibility is to describe resonances in terms of local integrals of motion (LIOM) [30,31], a hypothesized set of quasilocal operators that commute with one another and with the evolution operator. However, this approach creates a barrier to quantitative investigations because LIOM cannot be defined uniquely [32–36]. Additionally, schemes intended to construct them inevitably break down in the vicinity of the transition to the ergodic phase. It is therefore essential to develop a more complete understanding of resonances that does not rely on LIOM, and is instead based on quantities that are both computationally accessible and unambiguous. With this motivation, in this work we instead formulate our theory in terms of the matrix elements of local observables. These matrix elements can be calculated using standard numerical techniques.

This paper is organized as follows. In Sec. II we describe the idea of a many-body resonance. Following this, in Sec. III we discuss how their local structure can be captured

*sjgarratt@berkeley.edu
†sthitadhi.roy@icts.res.in

analytically. This leads us to the central result of this work in Sec. IV. There we show how the matrix elements of observables are related to energy splittings, and we calculate the distribution of energy scales governing dynamics in the MBL phase. The form of this distribution is elucidated through a resonance counting argument in Sec. V. Using these results, in Sec. VI we calculate the distribution of polarizations, and in Sec. VII that of fidelity susceptibilities. We summarize our results in Sec. VIII.

II. LOCAL RESONANCES

Before discussing resonances in MBL spin chains, it is helpful to first outline the origins and structure of Mott resonances in noninteracting Anderson insulators. We can imagine starting from a set of perfectly localized single-particle eigenstates on a lattice whose sites have random energies. Introducing weak hopping between neighboring sites, typical eigenstates acquire exponentially decaying tails in real space, but they remain well-localized. However, some pairs of sites will be sufficiently close in energy that they are strongly hybridized by the hopping, and the resulting eigenstates will have significant weight on each of the two sites involved. These resonances can be described approximately as two-level systems [23,25].

The MBL systems of interest here are spin chains in random local fields, and with weak short-range interactions on energy scale J. For $J = 0$, these are systems of decoupled spins, and we denote by $(h_j/2)\sigma_j$ the random local field operators, where $j = 1, \ldots, L$ labels the sites. The field strengths $h_j > 0$ are of order unity, and the local operators σ_j have eigenvalues ± 1. For $J = 0$, the eigenstates $|n\rangle$ of the evolution operator satisfy $\sigma_j |n\rangle = s_{n,j} |n\rangle$ with $s_{n,j} = \pm 1$, and here the LIOM are simply the operators σ_j. For small $J \neq 0$ it is expected that the LIOM are dressed by the interaction, and thereby develop exponentially-decaying tails in real space [30,31]. Their eigenvalues could then be used to label the eigenstates. In this sense, the eigenstates locally resemble those in the decoupled system. On the other hand, we know that if a pair of eigenstates are for $J = 0$ sufficiently close in energy, then when switching on the interaction $J \neq 0$ these states will be strongly hybridized. We refer to this situation as a many-body resonance.

The stability of the MBL phase relies on the fact that resonances are not simple two-level systems. Where there are two-dimensional resonant subspaces, these are embedded locally within pairs of many-body eigenstates. Previously this feature has been captured by appealing directly to pictures based on LIOM [15,19], and by considering the spectral properties of evolution operators defined on finite subregions [22,27], although each of those approaches suffers from a degree of ambiguity (this problem can of course be avoided by studying resonances on the scale of the system size [20,21]). Accounting for locality is essential because, even deep within the MBL phase, eigenstates are involved in an extensive number of local resonances. Here we describe local resonances in terms of the matrix elements of local observables, thereby isolating the participating degrees of freedom. This will allow us to describe the two-dimensional resonant subspaces in terms of local properties of many-body eigenstates.
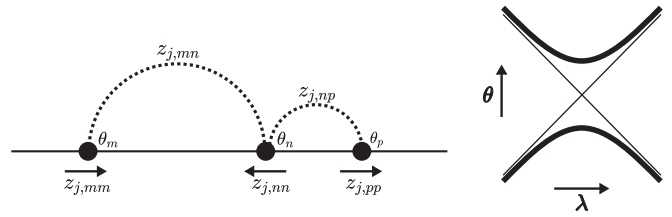

FIG. 1. Parametric dynamics induced by varying a local field $h_j(\lambda) = h_j + \lambda$, which couples to the local operator σ_j at site j. The parameter λ can be viewed as a fictitious time, and in the case of Floquet dynamics we denote by $e^{i\theta_n}$ the eigenvalues of the Floquet operator. Left: Three levels at a particular λ, with the θ axis horizontal. The diagonal matrix elements $z_{j,nn}$ of σ_j determine level velocities $\partial_\lambda \theta_n$, and off-diagonal matrix elements $z_{j,nm}$ increase in magnitude as levels approach resonance. Right: Thin lines show the level dynamics for a system with decoupled degrees of freedom, where an exact level crossing occurs as λ is varied, and thick lines correspond to the interacting case, where the crossing is avoided and corresponds to a resonance.

III. PARAMETRIC DYNAMICS

Our theoretical considerations are based on the effect of parametric variations of the disorder, which can be viewed as inducing dynamics of the spectral properties in a fictitious time; see Fig. 1 for a schematic visual. The idea is particularly powerful in this setting because the avoided crossings that arise under parametric dynamics can be identified with many-body resonances [22]. The parametric approach has a long history in studies of random matrices [37], semiclassical chaos [38–40], and disordered conductors [41–44], and more recently it has been applied in the context of MBL [13,45–49]. A common approximation is to decouple the parametric dynamics of eigenvalues from that of eigenstates, which is reasonable when eigenstates are almost featureless (such as in the ergodic phase). As in Ref. [22], we do not make this approximation. To understand the structure of resonances, it is essential to understand how eigenvalues and eigenstates are coupled with one another.

Using this idea, we will show how a two-dimensional resonant subspace can be described in terms of local properties of many-body eigenstates $|n\rangle$. First observe that for $J = 0$ the eigenstates are tensor products of eigenstates of each of the σ_j, so they are perfectly polarized along the field directions: $z_{j,nn} \equiv \langle n|\sigma_j|n\rangle = s_{n,j}$. Additionally, the off-diagonal matrix elements $z_{j,nm} \equiv \langle n|\sigma_j|m\rangle = 0$. Since the eigenvalues of the time evolution operator are for $J = 0$ determined by signed sums of local fields $\sum_j s_{n,j} h_j$, there is no level repulsion. If we consider a smooth variation of a single local field h_j, then for $J = 0$ there are many exact level crossings. For small $J \neq 0$, all of these exact level crossings are replaced by avoided crossings, as illustrated in Fig. 1. Moreover, in the vicinity of an avoided crossing between $|n\rangle$ and $|m\rangle$ induced by varying h_j, the off-diagonal matrix element $z_{j,nm}$ is of order unity [22]. Since $\sum_m |z_{j,nm}|^2 = \sum_n |z_{j,nm}|^2 = 1$, this implies that $z_{j,nn}$ and $z_{j,mm}$ are suppressed to well below unity, and therefore that near j the states $|n\rangle$ and $|m\rangle$ do not resemble the $J = 0$ eigenstates.

There are two classes of variations that must be distinguished. For $J = 0$ and focusing a particular level pair, varying the field $h_j(\lambda) = h_j + \lambda$ will either lead to an exact crossing of levels in the case $s_{n,j} = -s_{m,j}$, or otherwise cause them to move parallel to one another in the case $s_{n,j} = s_{m,j}$. While for small $J \neq 0$ the exact crossings are replaced by avoided ones, we do not expect a dramatic difference in behavior in the other case. Focus now on $|n\rangle$, $|m\rangle$, and a variation h_j that leads to an avoided crossing. We denote by $\omega^*_{j,nm}$ the minimum level separation, which occurs at fictitious time $\lambda = \lambda^*_{j,nm}$. With perturbation $(\lambda/2)\sigma_j$ we find

$$\partial_\lambda \omega_{nm} = y_{j,nm} \equiv (z_{j,nn} - z_{j,mm})/2,$$
$$\partial_\lambda |n\rangle = \frac{1}{2} \sum_{p \neq n} \omega^{-1}_{np} z_{j,pn} |p\rangle. \tag{1}$$

For Floquet systems, the factor ω^{-1}_{np} should be replaced by $i[1 - e^{-i\omega_{np}}]^{-1}$, but these coincide for $|\omega_{np}| \ll \pi$. We find for the matrix elements of σ_j,

$$\partial_\lambda z_{j,nm} = -\omega^{-1}_{nm} z_{j,nm} y_{j,nm} + \cdots,$$
$$\partial_\lambda y_{j,nm} = \omega^{-1}_{nm} |z_{j,nm}|^2 + \cdots, \tag{2}$$

where the ellipses represent contributions depending on $z_{j,np}$ and $z_{j,mp}$ for $p \neq m, n$. These contributions are significant only for states $|p\rangle$ that resonate with $|n\rangle$ or $|m\rangle$ at the site j, and in order to make analytic progress we neglect them in the first instance. This approximation that resonances are locally rare will be shown to be self-consistent below.

Within the approximation of decoupled local resonances, we find a closed system of differential equations that describe variations of ω_{nm} and of the matrix elements in Eq. (2). This set of equations simply describes an avoided crossing in a two-dimensional resonant subspace, but crucially is expressed only in terms of properties of the eigenstates $|n\rangle$ and $|m\rangle$ that are local to the site j. The solutions, which we discuss in Appendix B, are parametrized by three constants of integration. Two of these are $\lambda^*_{j,nm}$ and $\omega^*_{j,nm}$, and the third $R^2_{j,nm} \equiv y^2_{j,nm} + |z_{j,nm}|^2$ sets the scale of the variation of the matrix elements as the level pair passes through resonance. Since for $J = 0$ we have $R^2_{j,nm} = 1$, it is natural to expect that for $J \neq 0$ the constant $R^2_{j,nm}$ is reduced only by an amount of order J. It is straightforward to show that $\partial_\lambda(\omega_{nm} z_{j,nm}) = 0$ and

$$|z_{j,nm} \omega_{nm}| = |R_{j,nm} \omega^*_{j,nm}|. \tag{3}$$

As the splitting ω_{nm} passes through a minimum, the magnitude of the matrix element $z_{j,nm}$ passes through its maximum value of $R_{j,nm}$, and these two effects cancel with one another. For small J we expect the above to provide an approximate description of avoided crossings between essentially all level pairs, regardless of their separation in the spectrum. For example, the highest energy resonances correspond to $|z_{j,nm}| \sim 1$ for ω_{nm} that is exponentially larger in L than the mean level separation.

The conservation of $z_{j,nm} \omega_{nm}$ under variations of h_j within the approximation of decoupled resonances hints at interesting features in the spectral properties. Before discussing these, it is important to bear in mind that even within this

approximation, each of $z_{j,nm} \omega_{nm}$ and ω_{nm} depends on $h_{k \neq j}$. We will additionally assume that any variations of $z_{j,nm} \omega_{nm}$ and ω_{nm} that are induced by those of $h_{k \neq j}$ are uncorrelated. Crucially, we are not assuming that variations of $z_{j,nm}$ and ω_{nm} are uncorrelated; a change in the field h_k that brings $|n\rangle$ and $|m\rangle$ closer to a resonance that involves the site j will cause ω_{nm} to decrease and $|z_{j,nm}|$ to increase. Of course, outside of the approximation of decoupled resonances, there are also small variations of $z_{j,nm} \omega_{nm}$ with h_j, and we discuss these in Appendix C. In summary, within the above approximations, $z_{j,nm} \omega_{nm}$ and ω_{nm} are only weakly correlated with one another.

IV. ENERGY SCALES

An important feature of the MBL phase is that the energy scales associated with resonances have an extremely broad distribution [21,22]. Our arguments in the previous section show how these energy scales are encoded in the matrix elements $z_{j,nm}$ and in the level separations ω_{nm}. If we write

$$|z_{j,nm}| = \frac{\Omega_{j,nm}}{|\omega_{nm}|}, \tag{4}$$

then the ensemble-averaged distribution $p_\Omega(\Omega_{j,nm})$ of "resonant energy scales" $\Omega_{j,nm}$ is independent of ω_{nm} for $\Omega_{j,nm} < |\omega_{nm}|$. Given this distribution, one would have access to the correlations between $z_{j,nm}$ and ω_{nm}, and therefore the real-time dynamics of the local observable σ_j. For example, the infinite temperature autocorrelation function $C(t) = 2^{-L}\text{Tr}[\sigma_j(t)\sigma_j] = 2^{-L} \sum_{nm} |z_{j,nm}|^2 e^{-i\omega_{nm}t}$. The increase of $z_{j,nm}$ with decreasing ω_{nm} in Eq. (4) indicates that low-frequency oscillations have large amplitudes. On the other hand, the slow decrease of $z_{j,nm}$ with increasing ω_{nm} indicates that the potential for resonance is felt even for $|\omega_{nm}| \gg \Omega_{j,nm}$.

The correlations in Eq. (4) do not provide a prediction for $p_\Omega(\Omega)$, but they do provide a prescription for calculating it. Through exact diagonalization (ED) it is straightforward to obtain the eigenstates and eigenvalues of the evolution operator, compute $z_{j,nm}$ and ω_{nm}, and subsequently calculate the distribution of their product. We perform this analysis for a Floquet model for the MBL phase [50–52] that was used previously in Refs. [22,53]. This model appears to be MBL for $J \leqslant 0.07$, and we provide details in Appendix A. In Figs. 2(a) and 2(b), we show for small J that $p_\Omega(\Omega)$ decays as a power of Ω, and that for fixed Ω the distribution scales as $p_\Omega(\Omega) \propto 2^{-L}$. The exponential dependence on L is necessary for the system to be MBL at large L, as we discuss in Sec. VI. In Sec. V we rationalize the observed behavior of $p_\Omega(\Omega)$ using a heuristic resonance counting argument.

Equation (4) has predictive power because, as argued in Sec. III, the distribution of Ω is approximately independent of ω in the regime $\Omega_0 < \Omega < |\omega|$. Note that the lower cutoff Ω_0 must be exponentially small in L because p_Ω is proportional to 2^{-L} and decays as a power of Ω. To confirm the weak correlations between Ω and ω, in Figs. 2(c)–2(f) we compute the ensemble-averaged conditional distributions $p_{\Omega|\omega}(\Omega)$ for various ω. The collapse of $p_{\Omega|\omega}(\Omega)$ over several decades in both Ω and ω provides strong evidence that, when exploring the ensemble of MBL systems at a given J, variations of $z_{j,nm} \omega_{nm}$ and ω_{nm} are only weakly correlated. Since
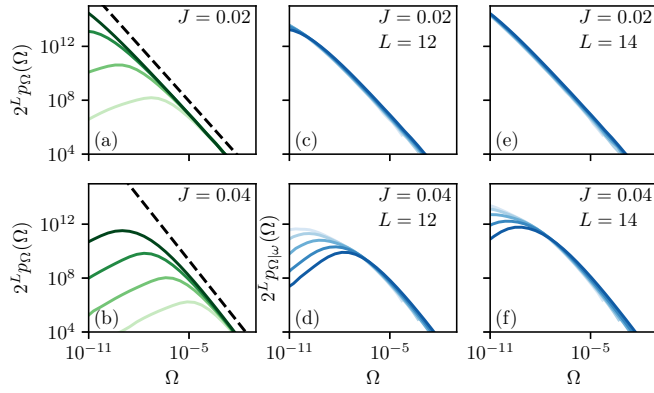
FIG. 2. (a),(b) Distribution p_Ω of Ω [Eq. (4)] for $L = 8, 10, 12, 14$ (increasing from light to dark) with (a) $J = 0.02$ and (b) $J = 0.04$. Dashed lines indicate power-law fits to p_Ω for $L = 14$, with exponents set by $\zeta/\zeta_c = 0.39(1)$ for $J = 0.02$ and $\zeta/\zeta_c = 0.61(4)$ for $J = 0.04$ [see Eq. (5)]. (c)–(f) Conditional distribution $p_{\Omega|\omega}(\Omega)$ of $\Omega < |\omega|$ within various windows of $|\omega|$. Windows are $|\omega| < 10^{-4}$ and $10^{-(n+1)} < |\omega| < 10^{-n}$ for $n = 0, 1, 2, 3$, with $|\omega|$ increasing from light to dark.

$p_{\Omega|\omega}(\Omega)$ is normalized, $\int_0^\omega d\Omega\, p_{\Omega|\omega}(\Omega) = 1$, small ω of course implies more weight at small Ω, and this effect is clear in Figs. 2(c)–2(f).

Comparing Eqs. (3) and (4), it is clear that $\Omega_{j,nm}$ has a rough interpretation as the minimum splitting between a pair of levels passing through an avoided crossing. The statistics of these splittings have been studied in chaotic systems for some time [54–56], although an important contrast is that in our case the pairs of levels passing through avoided crossings are not necessarily nearest neighbors; it is clear from Fig. 2 that there are resonant energy scales Ω that are much larger than the mean level spacing. We note that the energies associated with resonances on the scale of the system size L ("end-to-end" resonances) were determined in Ref. [21] by working with the many-body eigenstates themselves, as opposed to the matrix elements of local observables. There the approach is appropriate since for end-to-end resonances the appropriate two-dimensional subspaces are not locally embedded in many-body eigenstates, but are simply spanned by pairs of them.

V. RESONANCE COUNTING

Here we provide a rationalization of the behavior in Fig. 2. Starting from a system of decoupled qubits, for small J we suppose that it is possible to perform perturbation theory. Since this is a perturbation theory in a short-range interaction, we expect that each resonance can be associated with a length r, and that the corresponding energy scales $\sim e^{-r/\zeta}$, where the emergent quantity ζ is defined below (at small J, we expect $e^{-1/\zeta} \propto J$). If we choose to identify these energy scales with Ω defined in Eq. (4), we can estimate $p_\Omega(\Omega)$ via resonance counting. Note that for a given eigenstate and location in space, the number of possible resonances with length r grows as 2^r. Assuming that, for a given $r < L$, the various Ω are distributed between the respective lower and upper cutoffs

$\Omega_0 \sim e^{-L/\zeta}$ and $e^{-r/\zeta}$, we find a power-law distribution

$$p_\Omega(\Omega) = \frac{\zeta}{\zeta_c} \Omega_0^{\zeta/\zeta_c} \Omega^{-(1+\zeta/\zeta_c)} \sim 2^{-L} \Omega^{-(1+\zeta/\zeta_c)}, \quad (5)$$

which follows from weighting contributions from resonances with length r by 2^r. Here $\zeta_c \equiv [\ln 2]^{-1}$, $\Omega_0 < \Omega < e^{-1/\zeta}$, and $p_\Omega(\Omega) \to \delta(\Omega)$ as $J \to 0$. Note that the factor 2^{-L} here arose from the choice $\Omega_0 \sim e^{-L/\zeta}$.

There is evident agreement between the counting argument leading to Eq. (5) and the exact numerics used for Fig. 2, so it is convenient to view Eq. (5) as the definition of ζ. Both approaches lead to a power-law decay of $p_\Omega(\Omega)$ with Ω, with the exponent corresponding to $0 < \zeta/\zeta_c < 1$, and an exponential decay with L. Moreover, the values of ζ extracted from Figs. 2(a) and 2(b) (see the caption) are consistent with the results of Ref. [22]. From these estimates for ζ it can be verified that the power laws in Figs. 2(a) and 2(b) persist only down to $\Omega \simeq \Omega_0$, where the anticipated finite-size effects set in.

VI. LOCAL POLARIZATIONS

Having established the behavior in Eqs. (4) and (5), we now discuss the statistical properties of the matrix elements $z_{j,nm}$ without any energy resolution. First, we calculate the distribution of $Z_{j,nm} = |z_{j,nm}|^2$, which will allow us to check whether our initial assumption, that $Z_{j,nm}$ is typically much smaller than unity, is consistent with the results in the previous sections. Following this we investigate the distribution of polarisations $|z_{j,nn}|^2 = 1 - D_{j,n}$, where we have defined the depolarisation $D_{j,n}$ of $|n\rangle$ at site j. Because σ_j squares to the identity, we have

$$D_{j,n} \equiv 1 - Z_{j,nn} = \sum_{m \neq n} Z_{j,nm}. \quad (6)$$

Since a resonance between $|n\rangle$ and $|m\rangle$ at site j is characterized by a matrix element $z_{j,nm}$ of order unity, the number of such contributions to the sum in Eq. (6) is at most of order unity. For the MBL phase with $J \neq 0$ to resemble the $J = 0$ limit we expect that typically $D_{j,n} \ll 1$, which is a far more stringent condition than $Z_{j,nm} \ll 1$.

To understand the structure of Eq. (6) we compute the distributions $p_Z(Z_{j,nm})$ of $Z_{j,nm}$ and $p_D(D_{j,n})$ of $D_{j,n}$. The former is

$$p_Z(Z) = \langle \delta(Z - \Omega^2/\omega^2) \rangle, \quad (7)$$

where the angular brackets denote an average over ω and Ω. There is level repulsion on scales $|\omega| \sim \Omega$, but for $|\omega| \gg \Omega$ we can neglect correlations between ω and Ω. Treating ω as uniformly distributed in this regime, we find from the Jacobian $\partial \omega/\partial Z \sim \Omega Z^{-3/2}$ [see Eq. (4)] that for $\zeta < \zeta_c$ [22],

$$p_Z(Z) \sim 2^{-L} g(\zeta) Z^{-3/2}, \quad \Omega_0 \ll Z \ll 1, \quad (8)$$

up to a prefactor of order unity. The function $g(\zeta) = [\zeta_c - \zeta]^{-1} e^{[\zeta_c^{-1} - \zeta^{-1}]}$ increases with ζ and diverges as $\zeta \to \zeta_c$. From Eq. (8) it is clear that Z is typically much smaller than unity, as required for the approximation of decoupled resonances in Sec. III to be appropriate. For example, the mean $\langle Z \rangle \sim g(\zeta) 2^{-L}$. As an aside, we note that
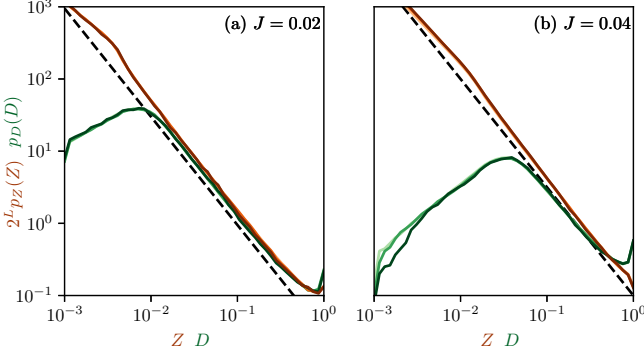
FIG. 3. Distributions of modulus-squared off-diagonal matrix elements $Z_{j,nm} = |z_{j,nm}|^2$ (oranges) and depolarizations $D_{j,n}$ (greens) for (a) $J = 0.02$ and (b) $J = 0.04$, and $L = 8, 10, 12$ (light to dark). Dashed lines indicate the power-law decay $Z^{-3/2}$ expected from Eq. (8).

the distribution of the matrix elements of σ_j has previously been characterized using an inverse participation ratio (IPR), which with exponent q is defined as $\sum_m Z_{j,nm}^q$ [11,57]. From the distribution Eq. (8) we see that the average IPRs are L-independent for $q > 1/2$.

Equation (8) shows that the average depolarization $\langle D \rangle \sim g(\zeta)$. Crucially, because $p_\Omega(\Omega) \propto 2^{-L}$ and $\zeta < \zeta_c$, $\langle D \rangle$ is finite in the thermodynamic limit. This is of course essential for the existence of a MBL phase. Neglecting correlations between the different terms $Z_{j,nm}$ in Eq. (6), we can additionally calculate the distribution of depolarizations $p_D(D)$. When $D_{j,n}$ is dominated by just one term in the sum, we have

$$p_D(D) \simeq 2^L p_Z(D) \sim g(\zeta) D^{-3/2}. \tag{9}$$

In Fig. 3 we compute $p_D(D)$ and $p_Z(Z)$ numerically, and we find excellent support for Eqs. (8) and (9) for sufficiently large Z and D. The result for $p_D(D)$ in Fig. 3 shows that the smallest polarizations are due to resonances, an $O(1)$ number of which dominate the sum in Eq. (6).

Interestingly, there is a "knee" in $p_Z(Z)$ in Fig. 3, below which $p_Z(Z)$ is larger than would be expected from Eq. (8). The origin of the knee can be understood by noting that, in calculating $p_Z(Z)$, there were two cases we should have distinguished. For half of the level pairs, the maximum Z on resonance is of order unity, and for the other half the maximum Z on resonance should vanish as $J \to 0$, so for small J we expect in the second case that the maximum $Z \sim J$. Another way to describe these two cases is to say that whereas in the first level repulsion restricts us to $|\omega| \gtrsim \Omega$, in the second we are restricted to $|\omega| \gtrsim \Omega/J$. Taking this into account in the calculation leading to Eq. (8) gives rise to the observed enhancement of $p_Z(Z)$ for $Z \lesssim J$ relative to $J \lesssim Z \leqslant 1$.

VII. RESPONSE TO PERTURBATIONS

Alongside the physical quantities discussed in the previous sections, another way to investigate resonances is by asking how many-body eigenstates respond to local perturbations. Here we focus on the fidelity susceptibility χ. This quantity was introduced as a probe of singular behavior at quantum

quantum transitions [58–60], and has more recently been investigated in the context of instabilities of the MBL phase and the onset of quantum chaos [12–18]. Following this, we revisit the level curvatures κ discussed in Refs. [13,22,46]. In each case, we will see that the statistical properties follow straightforwardly from the correlations in Eq. (4).

The fidelity susceptibility is defined here as $\chi_{j,n} \equiv 4|\partial_\lambda |n\rangle|^2$, where the additional factor of 4 will be convenient below. From perturbation theory, we have

$$\chi_{j,n} = \sum_{m \neq n} x_{j,nm}, \quad x_{j,nm} \equiv \frac{|z_{j,nm}|^2}{\omega_{nm}^2}. \tag{10}$$

The distribution $p_\chi(\chi_{j,n})$ of $\chi_{j,n}$ is extremely broad, and consequently it is often more instructive to investigate this directly instead of computing its moments. We will first determine the distribution $p_x(x_{j,nm})$ of $x_{j,nm}$, which is given by

$$p_x(x) = \langle \delta(x - \Omega^2 \omega^{-4}) \rangle, \tag{11}$$

where the angular brackets denote an average over Ω and ω, and we have used Eq. (4). This average is evaluated as a double integral over ω and $\Omega < |\omega|$, which proceeds as follows. For resonances on energy scale Ω, the contribution to $p_x(x)dx$ from frequencies within $d\omega$ of $\omega = \Omega^{1/2} x^{-1/4}$ is $\sim \Omega^{1/2} x^{-5/4} dx$, where we have used the fact that the ω distribution is approximately uniform for $|\omega| > \Omega$. The restriction $\Omega < |\omega|$ corresponds to $\Omega < x^{-1/2}$, and integrating over resonances on all scales, we have for $x \gg 1$,

$$p_x(x) \sim 2^{-L} x^{-5/4} \int_{\Omega_0}^{x^{-1/2}} d\Omega\, \Omega^{-(1/2 + \zeta/\zeta_c)} \tag{12}$$

from Eq. (5). This expression highlights a change in behavior at $\zeta/\zeta_c = 1/2$. Deep within the MBL phase with $\zeta/\zeta_c < 1/2$ the integral over Ω is dominated by resonances with $\Omega \sim x^{-1/2}$, and this leads to

$$p_x(x) \sim 2^{-L} x^{-(3 - \zeta/\zeta_c)/2}. \tag{13}$$

For $\zeta/\zeta_c < 1/2$, the distribution is controlled by pairs of levels close to resonance at j, in the sense that the off-diagonal matrix elements of σ_j are large. For $\zeta/\zeta_c > 1/2$, on the other hand, the integral is dominated by contributions from resonances on the finest energy scales $\Omega \sim \Omega_0$ throughout the entire window $1 \ll x \ll \Omega_0^{-2}$. Note that this implies contributions from pairs of levels that may be very far from resonance at j, having $|\omega| \gg \Omega_0$. In this regime, there is also a change in the scaling with L, and from Eqs. (4) and (5) we find $p_x(x) \sim e^{-L/(2\zeta)} x^{-5/4}$. Note, however, that Fig. 2 as well as Ref. [21] indicate that finite-size effects modify the distribution $p_\Omega(\Omega)$ relative to Eq. (5) for $\Omega \lesssim \Omega_0$, so in the following we restrict our analytic considerations to $\zeta/\zeta_c < 1/2$.

Since χ is a sum of $\sim 2^L$ of the quantities x, it is straightforward to determine $p_\chi(\chi)$ in the regime where a single term dominates the sum. In that case, $p_\chi(\chi) \simeq 2^L p_x(\chi)$. When $\zeta/\zeta_c < 1/2$ this occurs for χ larger than an L-independent threshold. We then find

$$p_\chi(\chi) \sim \chi^{-(3 - \zeta/\zeta_c)/2}. \tag{14}$$

The slow decay of $p_\chi(\chi)$ with increasing χ shows clearly that the mean $\int d\chi\, p_\chi(\chi)\chi$ is controlled by resonances with $\Omega \sim \Omega_0$ [12,14,15]. However, such resonances do not affect
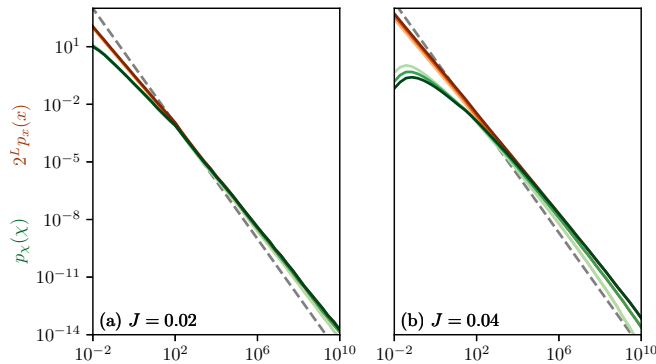
FIG. 4. Distributions $2^L p_x(x)$ (oranges) and $p_\chi(\chi)$ (greens) for (a) $J = 0.02$ and (b) $J = 0.04$, and $L = 8, 10, 12$ (light to dark). Dashed lines indicate the power-law decay $\chi^{-3/2}$ expected for systems with Poissonian spectra.

dynamics on physical timescales, highlighting the necessity of focusing instead on the full distribution.

The result Eq. (14) illustrates the role of the correlations between the matrix elements $z_{j,nm}$ and the level separations ω_{nm}. It should be contrasted with the distributions $p_\chi(\chi) \sim \chi^{-(3+\beta)/2}$ obtained for systems with Poissonian spectra ($\beta = 0$) and random matrices drawn from the orthogonal ($\beta = 1$) and unitary ($\beta = 2$) ensembles [12]. This dependence on the level-repulsion exponent β can be seen to follow from (i) treating $z_{j,nm}$ as independent of ω_{nm}, and (ii) the distribution of level separations $p_\omega(\omega) \sim |\omega|^\beta$ for ω below the mean level spacing. The results of this work, in particular those in Sec. IV, clearly demonstrate that the first of these steps is inappropriate in MBL systems. Indeed, from Eq. (14) we expect a decay of $p_\chi(\chi)$ slower than $\chi^{-3/2}$, but comparing with the random-matrix result $p_\chi(\chi) \sim \chi^{-(3+\beta)/2}$ appears to indicate an "effective" $\beta < 0$. Neglecting the correlations between $z_{j,nm}$ and ω_{nm} could then lead to the erroneous conclusion $p_\omega(\omega) \sim |\omega|^{-\zeta/\zeta_c}$ at small ω, i.e., "level attraction" [14], the absence of which is a central assumption in the proof of MBL in one dimension [27]. Here we have shown that a decay of $p_\chi(\chi)$ slower than $\chi^{-3/2}$ arises in the case in which there is only level repulsion, which becomes stronger for larger ζ/ζ_c [22]. At the heart of this calculation is the fact that $z_{j,nm}$ and ω_{nm} are strongly correlated, and that these correlations are characterized by the power-law distribution in Eq. (5).

In Fig. 4 we compute $p_x(x)$ and $p_\chi(\chi)$ numerically. Since we perform these calculations for a Floquet model, the denominator ω_{nm}^2 in Eq. (10) is replaced by $(2 \sin[\omega_{nm}/2])^2$, which follows from perturbation theory for Floquet operators as opposed to Hamiltonian ones. For large χ we find excellent agreement between $p_\chi(\chi)$ and $2^L p_x(\chi)$, showing that the sum $\chi_{j,n} = \sum_{m \neq n} x_{j,nm}$ is dominated by the largest term. The distributions determined numerically follow power laws over many decades in χ, and the observed decay is marginally slower than $\chi^{-3/2}$, as expected from Eq. (14).

Instead of discussing the overlaps of perturbed and unperturbed many-body eigenstates, we can also ask about changes in the expectation values of local observables. In particular, we can ask how $z_{j,nn}$ varies with the field h_j. It is an exercise in second-order perturbation theory to show that the result is

proportional to the level curvature $\kappa_{j,n}$. For convenience we define $\kappa_{j,n} = \partial_\lambda z_{j,nn}$, so that

$$\kappa_{j,n} = \sum_{m \neq n} k_{j,nm}, \quad k_{j,nm} \equiv \frac{|z_{j,nm}|^2}{\omega_{nm}}, \quad (15)$$

and it is important to note that these quantities can have either sign. The calculation of $p_\kappa(\kappa)$ is similar to that of $p_\chi(\chi)$. For $\zeta/\zeta_c < 2/3$, the distribution $p_k(k)$ of k is controlled by levels with $\omega \sim \Omega$, and so with $\Omega \sim |k|^{-1}$. For $\zeta/\zeta_c > 2/3$ it is controlled by $\Omega \sim \Omega_0$, and the L-dependence of the distribution is altered. For $\zeta/\zeta_c < 2/3$, we find

$$p_\kappa(\kappa) \sim |\kappa|^{-(2-\zeta/\zeta_c)}, \quad (16)$$

previously derived in Ref. [22]. The power law obtained there follows simply from the correlations in Eq. (4) and the distribution of resonant energy scales in Fig. 2 and Eq. (5).

Again we should contrast this distribution with the result for random matrices. For matrix elements of σ_j that are independent of level separations, having $p_\omega(\omega) \sim |\omega|^\beta$ for small ω, one instead finds $p_\kappa(\kappa) \sim |\kappa|^{-(2+\beta)}$ [61–64]. For each of $p_\chi(\chi)$ and $p_\kappa(\kappa)$, increasing the level repulsion exponent leads in the random-matrix setting to a faster power-law decay of the distribution, whereas in MBL systems increasing ζ/ζ_c (and hence the degree of level repulsion) leads to a slower power-law decay of the distribution. For large ζ/ζ_c, however, there is a distinct change in the distributions $p_\chi(\chi)$ and $p_\kappa(\kappa)$, which merits further investigation.

VIII. SUMMARY

To summarize, we have formulated a theory for resonances in the MBL phase in terms of local observables. A contrast between our study and previous ones is that we have described resonances not in terms of LIOM [15,19,21,22], but instead in terms of quantities that can be calculated using standard techniques. This allows for approximate analytic calculations that can be compared directly with numerics based on exact diagonalization. A key ingredient in our theory is the relation between matrix elements and the many-body level spectrum, which we have argued can be understood based on parametric dynamics. This relation highlights the fact that signatures of resonance on energy scale Ω are evident even for level pairs separated in the spectrum by $|\omega| \gg \Omega$. Using this, we have shown how the resonant energy scales are encoded in the statistics of matrix elements, and this has allowed us to demonstrate numerically that they have a power-law distribution. This distribution should be contrasted with the one calculated in Ref. [21] for pairs of states that are nearby on the scale of the mean level spacing. Our focus, as in Ref. [22], has been on finite energy scales, which corresponds to dynamics on finite time scales.

We have additionally determined the form of the tail in the distribution of polarizations, which have been studied extensively in MBL spin chains since Ref. [65]. A complementary perspective comes from asking not about the statistical properties of individual systems, but instead asking how systems respond to local perturbation [12,14,15]. To investigate this, we have determined, both analytically and numerically, the

distribution of eigenstate fidelity susceptibilities. Strikingly, this has uncovered a regime in which essentially the entire distribution is controlled by resonances on the finest energy scales, which are generally expected to correspond to extensive length scales. Our results also highlight an important difference relative to the behavior of ergodic systems and random matrices, namely that increasing the degree of level repulsion in an MBL system leads to a slower power-law decay of this distribution rather than a faster one. The origin of this effect is in the extremely broad distributions of matrix elements of local observables. A similar contrast with random matrices is present when considering how eigenstate expectation values of local observables respond to perturbations. This is quantified in part by the distribution of level curvatures, calculated in MBL systems in Refs. [13,22,46]. In this work, we have shown that this distribution, as well as the distribution of fidelity susceptibilities, follows from the correlations between matrix elements and the level spectrum in Eq. (4), and the power-law distribution of resonant energy scales in Eq. (5) and Fig. 2.

The observed power-law distribution is consistent with a counting argument based on independent local resonances, expected to be appropriate deep within the MBL phase. Since we have shown how to calculate the resonant energy scales explicitly, our numerical approach can be immediately extended to investigate resonances closer to the transition to ergodic behavior. An initial theoretical question in that regime concerns the statistics of the energy scales when high-energy resonances (corresponding to short lengthscales) can no longer be treated as independent. One possibility is to approach this problem by considering a hierarchical diagonalization procedure, whereby one accounts for resonances at successively lower energy scales. This idea has precedents in the study of the critical Anderson problem [66–69], where it was shown how the energy scales governing dynamics must flow, and it underlies the demonstration of MBL behavior in Ref. [27]. Very recently, a procedure of this kind has been implemented numerically [70]. Looking further afield, one might hope to extend the approach to develop a theoretical understanding of the percolation of resonances, which is expected to drive the transition [21,28,29].

APPENDIX A: FLOQUET MODEL

Here we describe the Floquet model for the MBL phase used for numerical calculations. In our models all points in the spectrum of the Floquet operator W are statistically equivalent, and there are no conserved densities. For integer time t the unitary evolution operator is W^t, and $W |n\rangle = e^{i\theta_n} |n\rangle$, where the quasienergies $\theta_n \in [-\pi, \pi)$. The Floquet operators that we use have the structure of brickwork quantum circuits, specifically $W = [\bigotimes_{j\,\text{odd}} w_{j,j+1}][\bigotimes_{j\,\text{even}} w_{j,j+1}]$, where $w_{j,j+1} = \exp[i\pi J \Sigma_{j,j+1}][u_j \otimes v_{j+1}]$. Here $\Sigma_{j,j+1}$ is the swap operator, or equivalently a Heisenberg coupling, acting on qubits j and $j+1$, while J is the coupling strength. The independent Haar-random 2×2 unitary matrices u_j and v_j describe the random fields, and due to these fields our model does not have time-reversal symmetry. Up to an overall phase, we can write $v_j u_j$ $(u_j v_j)$ for j even (odd) as $e^{i\vec{h}_j \cdot \vec{\sigma}_j/2} \equiv e^{ih_j \sigma_j/2}$, where $\vec{\sigma}_j$ is a vector of Pauli matrices and $h_j \equiv |\vec{h}_j|$ so that σ_j has eigenvalues ± 1. We restrict ourselves to behavior deep within the MBL phase, and so with J well below 0.07 [53]. Note that with periodic boundary conditions, the structure of the evolution operator necessitates L even.

APPENDIX B: SOLUTION OF PARAMETRIC EQUATIONS

Here we outline the solution of the system of equations in Eq. (2). For brevity we drop indices, e.g., $z = z_{j,nm}$, and shift the phase of z so that it is real. Then

$$\partial_\lambda \omega = y, \quad \partial_\lambda y = \omega^{-1} z^2, \quad \partial_\lambda z = -\omega^{-1} yz, \qquad \text{(B1)}$$

which describe an avoided crossing in a two-dimensional resonant subspace. In contrast with Ref. [22], it has not been necessary to introduce operators that describe the dynamics of subsystems, although Eqs. (B1) can also be derived using that approach. As discussed in the main text, solutions to Eqs. (B1) are parametrized by three constants of integration. Two of these are λ^* and ω^*, which can be identified with the fictitious time and splitting at the resonance, respectively. The third constant of integration is $R^2 \equiv y^2 + z^2$. Note that for $J = 0$ we necessarily have $z = 0$, while $y^2 = 0$ or 1, corresponding to level pairs that have the same or opposite polarizations at the site of the perturbation. For small $J \neq 0$, we therefore expect level pairs to have either R^2 of order J, or $R^2 = 1 - O(J)$.

To solve Eqs. (B1), it is convenient to write $y(\lambda) = -R \cos\varphi(\lambda)$ and $z(\lambda) = R \sin\varphi(\lambda)$. This leads to

$$\tan\varphi(\lambda) = \frac{\omega^*}{R(\lambda^* - \lambda)},$$
$$\omega^2(\lambda) = R^2(\lambda - \lambda^*)^2 + (\omega^*)^2, \qquad \text{(B2)}$$

which gives matrix elements of σ_j set by

$$y(\lambda) = \frac{R(\lambda^* - \lambda)}{\omega(\lambda)}, \quad z(\lambda) = \frac{R\omega^*}{\omega(\lambda)}. \qquad \text{(B3)}$$

Setting $\lambda = 0$ in the second of Eqs. (B3), we arrive at Eq. (4), and we identify $\Omega = R\omega^*$. In the case $R^2 = 1 - O(J)$, the energy scale Ω that controls the off-diagonal matrix elements of the local observable σ_j is approximately equal to the minimum level separation ω^* that arises under variations in λ.
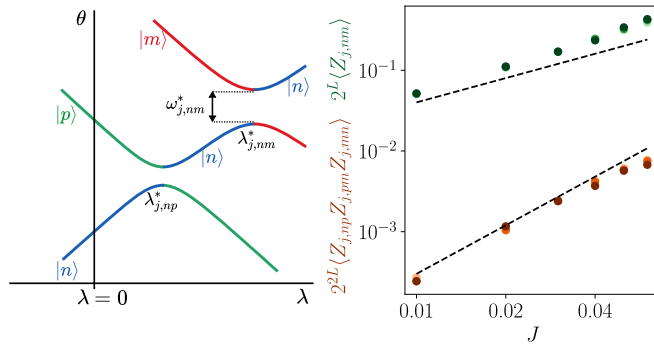
FIG. 5. Left: Diagram of parametric dynamics with three levels, with quasienergy θ vertical and fictitious time λ horizontal. The exchange of labels at avoided crossings is described after Eq. (B3). Right: Comparison of (greens) two-level $\langle Z_{j,nm} \rangle$ and (oranges) three-level $\langle Z_{j,np} Z_{j,pm} Z_{j,mn} \rangle$ terms for $L = 8, 10, 12$ (increasing from light to dark). Dashed lines indicate growth with J and with J^2.

APPENDIX C: VARIATIONS OF Ω

Moving beyond a two-dimensional resonant subspace, here we consider applying our theory to the full spectrum; aspects of this are discussed elsewhere [22]. First, it is necessary to adopt a convention for the relabeling of levels. The simplest choice is to exchange the labels of levels at the centers of avoided crossings, as illustrated in Fig. 5(a). In this way, the polarizations $z_{j,nn}$ have the same signs on both sides of these crossings. Second, we must ask how and whether $\Omega_{j,nm} = |\omega_{j,nm} z_{j,nm}|$ varies with λ once we account for coupling to levels $|p\rangle \neq |n\rangle, |m\rangle$.

This coupling can be analyzed within perturbation theory in λ. Variations of the energy scale $\Omega_{j,nm}$ are given by

$$\partial_\lambda \Omega_{j,nm}^2 = \sum_{p \neq n,m} f_{j,nmp}(z_{j,np} z_{j,pm} z_{j,mn} + \text{c.c.}),$$

$$f_{j,nmp} = \frac{1}{2} \omega_{j,nm}^2 \left[\omega_{j,mp}^{-1} + \omega_{j,np}^{-1} \right]. \tag{C1}$$

For Eq. (4) to be appropriate even for $|\omega_{nm}| \gg \Omega_{j,nm}$, the net variation in the resonant energy scale $\Omega_{j,nm}$ from fictitious time $\lambda_{j,nm}^*$ to the random realization $\lambda = 0$ of interest must be small. To understand how this can be the case, it is simplest to consider a level $|p\rangle$ with $R_{j,np}^2$ of order unity. This scenario is illustrated on the left in Fig. 5. Note that although the factor $\omega_{j,pn}^{-1}$ appearing in $f_{j,nmp}$ can be large, due to the above relabeling scheme it has opposite signs for $\lambda < \lambda_{j,np}^*$ and $\lambda > \lambda_{j,np}^*$. This means that a decrease in $\Omega_{j,nm}^2$ on one side of the resonance between $|n\rangle$ and $|p\rangle$ is (approximately) compensated by an increase on the other side. The net variation in $\Omega_{j,nm}$ is therefore suppressed.

An interesting effect beyond our two-level approximation appears in the quantity $z_{j,np} z_{j,pm} z_{j,mn}$ in Eq. (C1), and we now briefly discuss its modulus square, $Z_{j,np} Z_{j,pm} Z_{j,mn}$. In particular, these three matrix elements are not independent of one another. Suppose, as above, that $R_{j,mn}^2$ and $R_{j,np}^2$ are both of order unity while $R_{j,pm}^2$ is of order J. For such a set of levels we have $\langle Z_{j,mn} \rangle, \langle Z_{j,np} \rangle \sim 2^{-L} J$, while $\langle Z_{j,pm} \rangle \sim 2^{-L} J^2$. If we neglect correlations between these matrix elements, the disorder-average $\langle Z_{j,np} Z_{j,pm} Z_{j,mn} \rangle \sim 2^{-3L} J^4$. However, if there is a resonance between $|n\rangle$ and each of $|m\rangle$ and $|p\rangle$, this causes $Z_{j,pm}$ to acquire a value of order unity. As a consequence, we instead have $\langle Z_{j,np} Z_{j,pm} Z_{j,mn} \rangle \sim 2^{-2L} J^2$, and in Fig. 5 we confirm this behavior numerically. The J^2 scaling nevertheless reflects the rarity of three-level relative to two-level resonances.

[1] J. M. Deutsch, Quantum statistical mechanics in a closed system, Phys. Rev. A **43**, 2046 (1991).

[2] M. Srednicki, Chaos and quantum thermalization, Phys. Rev. E **50**, 888 (1994).

[3] M. Rigol, V. Dunjko, and M. Olshanii, Thermalization and its mechanism for generic isolated quantum systems, Nature (London) **452**, 854 (2008).

[4] L. D'Alessio, Y. Kafri, A. Polkovnikov, and M. Rigol, From quantum chaos and eigenstate thermalization to statistical mechanics and thermodynamics, Adv. Phys. **65**, 239 (2016).

[5] J. M. Deutsch, Eigenstate thermalization hypothesis, Rep. Prog. Phys. **81**, 082001 (2018).

[6] I. V. Gornyi, A. D. Mirlin, and D. G. Polyakov, Interacting Electrons in Disordered Wires: Anderson Localization and Low-T Transport, Phys. Rev. Lett. **95**, 206603 (2005).

[7] D. Basko, I. Aleiner, and B. Altshuler, Metal-insulator transition in a weakly interacting many-electron system with localized single-particle states, Ann. Phys. (NY) **321**, 1126 (2006).

[8] V. Oganesyan and D. A. Huse, Localization of interacting fermions at high temperature, Phys. Rev. B **75**, 155111 (2007).

[9] R. Nandkishore and D. A. Huse, Many-body localization and thermalization in quantum statistical mechanics, Annu. Rev. Condens. Matter Phys. **6**, 15 (2015).

[10] D. A. Abanin, E. Altman, I. Bloch, and M. Serbyn, Colloquium: Many-body localization, thermalization, and entanglement, Rev. Mod. Phys. **91**, 021001 (2019).

[11] M. Serbyn, Z. Papić, and D. A. Abanin, Thouless energy and multifractality across the many-body localization transition, Phys. Rev. B **96**, 104201 (2017).

[12] P. Sierant, A. Maksymov, M. Kuś, and J. Zakrzewski, Fidelity susceptibility in gaussian random ensembles, Phys. Rev. E **99**, 050102(R) (2019).

[13] A. Maksymov, P. Sierant, and J. Zakrzewski, Energy level dynamics across the many-body localization transition, Phys. Rev. B **99**, 224202 (2019).

[14] D. Sels and A. Polkovnikov, Dynamical obstruction to localization in a disordered spin chain, Phys. Rev. E **104**, 054105 (2021).

[15] P. J. D. Crowley and A. Chandran, A constructive theory of the numerically accessible many-body localized to thermal crossover, Sci. Post Phys. **12**, 201 (2022).

[16] M. Pandey, P. W. Claeys, D. K. Campbell, A. Polkovnikov, and D. Sels, Adiabatic Eigenstate Deformations as a Sensitive Probe for Quantum Chaos, Phys. Rev. X **10**, 041017 (2020).

[17] T. LeBlond, D. Sels, A. Polkovnikov, and M. Rigol, Universality in the onset of quantum chaos in many-body systems, Phys. Rev. B **104**, L201117 (2021).

[18] P. J. D. Crowley and A. Chandran, Partial thermalisation of a two-state system coupled to a finite quantum bath, Sci. Post Phys. **12**, 103 (2022).

[19] S. Gopalakrishnan, M. Müller, V. Khemani, M. Knap, E. Demler, and D. A. Huse, Low-frequency conductivity in many-body localized systems, Phys. Rev. B **92**, 104202 (2015).

[20] B. Villalonga and B. K. Clark, Eigenstates hybridize on all length scales at the many-body localization transition, arXiv:2005.13558 [cond-mat.dis-nn].

[21] A. Morningstar, L. Colmenarez, V. Khemani, D. J. Luitz, and D. A. Huse, Avalanches and many-body resonances in many-body localized systems, Phys. Rev. B **105**, 174205 (2022).

[22] S. J. Garratt, S. Roy, and J. T. Chalker, Local resonances and parametric level dynamics in the many-body localized phase, Phys. Rev. B **104**, 184203 (2021).

[23] N. F. Mott, Conduction in non-crystalline systems, Philos. Mag. **17**, 1259 (1968).

[24] V. L. Berezinskii, Kinetics of a quantum particle in a one-dimensional random potential, Zh. Eksp. Teor. Fiz. **65**, 1251 (1973) [Sov. Phys. JETP **38**, 620 (1974)].

[25] D. A. Ivanov, M. A. Skvortsov, P. M. Ostrovsky, and Y. V. Fominov, Hybridization of wave functions in one-dimensional localization, Phys. Rev. B **85**, 035109 (2012).

[26] L. Colmenarez, P. A. McClarty, M. Haque, and D. J. Luitz, Statistics of correlation functions in the random Heisenberg chain, Sci. Post Phys. **7**, 064 (2019).

[27] J. Z. Imbrie, Diagonalization and Many-Body Localization for a Disordered Quantum Spin Chain, Phys. Rev. Lett. **117**, 027201 (2016).

[28] W. De Roeck and J. Z. Imbrie, Many-body localization: stability and instability, Philos. Trans. R. Soc. A **375**, 20160422 (2017).

[29] W. De Roeck and F. Huveneers, Stability and instability towards delocalization in many-body localization systems, Phys. Rev. B **95**, 155129 (2017).

[30] M. Serbyn, Z. Papić, and D. A. Abanin, Local Conservation Laws and the Structure of the Many-Body Localized States, Phys. Rev. Lett. **111**, 127201 (2013).

[31] D. A. Huse, R. Nandkishore, and V. Oganesyan, Phenomenology of fully many-body-localized systems, Phys. Rev. B **90**, 174202 (2014).

[32] J. Z. Imbrie, V. Ros, and A. Scardicchio, Local integrals of motion in many-body localized systems, Ann. Phys. **529**, 1600278 (2017).

[33] V. Ros, M. Müller, and A. Scardicchio, Integrals of motion in the many-body localized phase, Nucl. Phys. B **891**, 420 (2015).

[34] A. Chandran, I. H. Kim, G. Vidal, and D. A. Abanin, Constructing local integrals of motion in the many-body localized phase, Phys. Rev. B **91**, 085425 (2015).

[35] L. Rademaker and M. Ortuño, Explicit Local Integrals of Motion for the Many-Body Localized State, Phys. Rev. Lett. **116**, 010404 (2016).

[36] D. Pekker, B. K. Clark, V. Oganesyan, and G. Refael, Fixed Points of Wegner-Wilson Flows and Many-Body Localization, Phys. Rev. Lett. **119**, 075701 (2017).

[37] F. J. Dyson, A Brownian-motion model for the eigenvalues of a random matrix, J. Math. Phys. **3**, 1191 (1962).

[38] P. Pechukas, Distribution of Energy Eigenvalues in the Irregular Spectrum, Phys. Rev. Lett. **51**, 943 (1983).

[39] T. Yukawa, New Approach to the Statistical Properties of Energy Levels, Phys. Rev. Lett. **54**, 1883 (1985).

[40] K. Nakamura and M. Lakshmanan, Complete Integrability in a Quantum Description of Chaotic Systems, Phys. Rev. Lett. **57**, 1661 (1986).

[41] A. Szafer and B. L. Altshuler, Universal Correlation in the Spectra of Disordered Systems with an Aharonov-Bohm Flux, Phys. Rev. Lett. **70**, 587 (1993).

[42] B. D. Simons and B. L. Altshuler, Universal Velocity Correlations in Disordered and Chaotic Systems, Phys. Rev. Lett. **70**, 4063 (1993).

[43] B. D. Simons and B. L. Altshuler, Universalities in the spectra of disordered and chaotic systems, Phys. Rev. B **48**, 5422 (1993).

[44] J. T. Chalker, I. V. Lerner, and R. A. Smith, Random Walks through the Ensemble: Linking Spectral Statistics with Wave-Function Correlations in Disordered Metals, Phys. Rev. Lett. **77**, 554 (1996).

[45] M. Serbyn and J. E. Moore, Spectral statistics across the many-body localization transition, Phys. Rev. B **93**, 041424(R) (2016).

[46] M. Filippone, P. W. Brouwer, J. Eisert, and F. von Oppen, Drude weight fluctuations in many-body localized systems, Phys. Rev. B **94**, 201112(R) (2016).

[47] C. Monthus, Level repulsion exponent β for many-body localization transitions and for Anderson localization transitions via Dyson Brownian motion, J. Stat. Mech. (2016) 033113.

[48] C. Monthus, Many-body-localization transition: sensitivity to twisted boundary conditions, J. Phys. A **50**, 095002 (2017).

[49] B. De, P. Sierant, and J. Zakrzewski, On intermediate statistics across many-body localization transition, J. Phys. A **55**, 014001 (2022).

[50] A. Lazarides, A. Das, and R. Moessner, Fate of Many-Body Localization Under Periodic Driving, Phys. Rev. Lett. **115**, 030402 (2015).

[51] P. Ponte, Z. Papić, F. Huveneers, and D. A. Abanin, Many-Body Localization in Periodically Driven Systems, Phys. Rev. Lett. **114**, 140401 (2015).

[52] L. Zhang, V. Khemani, and D. A. Huse, A Floquet model for the many-body localization transition, Phys. Rev. B **94**, 224202 (2016).

[53] S. J. Garratt and J. T. Chalker, Many-Body Delocalization as Symmetry Breaking, Phys. Rev. Lett. **127**, 026802 (2021).

[54] M. Wilkinson, Statistics of multiple avoided crossings, J. Phys. A **22**, 2795 (1989).

[55] J. Zakrzewski and M. Kuś, Distributions of Avoided Crossings for Quantum Chaotic Systems, Phys. Rev. Lett. **67**, 2749 (1991).

[56] J. Zakrzewski, D. Delande, and M. Kuś, Parametric motion of energy levels in quantum chaotic systems. II. Avoided-crossing distributions, Phys. Rev. E **47**, 1665 (1993).

[57] C. Monthus, Many-body-localization transition: strong multi-fractality spectrum for matrix elements of local operators, J. Stat. Mech. (2016) 073301.

[58] S. Sachdev, *Quantum Phase Transitions*, 2nd ed. (Cambridge University Press, Cambridge, 2011).

[59] P. Zanardi and N. Paunković, Ground state overlap and quantum phase transitions, Phys. Rev. E **74**, 031123 (2006).

[60] W.-L. You, Y.-W. Li, and S.-J. Gu, Fidelity, dynamic structure factor, and susceptibility in critical phenomena, Phys. Rev. E **76**, 022101 (2007).

[61] P. Gaspard, S. A. Rice, H. J. Mikeska, and K. Nakamura, Parametric motion of energy levels: Curvature distribution, Phys. Rev. A **42**, 4015 (1990).

[62] J. Zakrzewski and D. Delande, Parametric motion of energy levels in quantum chaotic systems. I. Curvature distributions, Phys. Rev. E **47**, 1650 (1993).

[63] F. von Oppen, Exact Distribution of Eigenvalue Curvatures of Chaotic Quantum Systems, Phys. Rev. Lett. **73**, 798 (1994).

[64] Y. V. Fyodorov and H.-J. Sommers, Universality of level curvature distribution for large random matrices: systematic analytical approaches, Z. Phys. B **99**, 123 (1995).

[65] A. Pal and D. A. Huse, Many-body localization phase transition, Phys. Rev. B **82**, 174411 (2010).

[66] L. S. Levitov, Delocalization of Vibrational Modes caused by Electric Dipole Interaction, Phys. Rev. Lett. **64**, 547 (1990).

[67] L. Levitov, Critical Hamiltonians with long range hopping, Ann. Phys. (Berlin) **511**, 697 (1999).

[68] A. D. Mirlin and F. Evers, Multifractality and critical fluctuations at the Anderson transition, Phys. Rev. B **62**, 7920 (2000).

[69] Y. V. Fyodorov, A. Kupiainen, and C. Webb, Towards rigorous analysis of the Levitov–Mirlin–Evers recursion, Nonlinearity **29**, 3871 (2016).

[70] D. M. Long, P. J. D. Crowley, V. Khemani, and A. Chandran, Phenomenology of the prethermal many-body localized regime, arXiv:2207.05761.